

When Black Holes Relax in a Cold Bath: Evolving Page Curves for Black Holes Coupled to Cooling Baths

Waheed A. Dar*

*Department of Physics
National Institute of Technology Srinagar,
Kashmir-190006, India*

Nirmalya Kajuri[†] and Rinkesh Panigrahi[‡]

*School of Physical Sciences,
Indian Institute of Technology Mandi,
Himachal Pradesh, India*

(Dated: July 1, 2025)

We consider scenarios where Jackiw-Teitelboim black holes are attached to baths whose temperatures can be manipulated externally. We consider the bath to be cooled continuously and numerically investigate the subsequent evolution of the generalized entropies of the black hole. Page curves corresponding to several different cooling profiles of the bath are obtained.

I. INTRODUCTION

The apparent loss of unitarity during black hole evaporation (aka the black hole information paradox) has remained one of the most profound challenges in attempting to reconcile quantum mechanics with gravity. A crucial insight [1] was that for black hole evaporation to be unitary, the entanglement entropy of radiation should initially increase but eventually decrease, following what is now known as the Page curve. It was only recently shown that at least for certain black holes, the entanglement entropy during evaporation indeed follows the Page curve [2, 3].

In [2], for example, the set-up considered was a two-dimensional black hole in Jackiw-Teitelboim gravity attached to a bath. By computing the quantum extremal surface via the generalized entropy formula of Engelhardt and Wall [4], it was found that there are two extremal surfaces that correspond to two saddles of the gravitational path integral—the Hawking saddle and the island saddle. A switch between the saddles takes place at Page time, and the Page curve is recovered. Since these breakthroughs, a deeper understanding of the transition has been obtained in terms of replica wormholes [5–7]. Building on these developments, there have been many investigations of Page curves for various black holes [8–19].

Generally, the evaporation of a black hole will be influenced by external conditions, such as ambient temperature or energy exchange with other systems. It is interesting to ask how changing the external conditions affects the Page curve? In this paper, we address this question for black holes in JT gravity, where we can model the changing external conditions by changing the bath temperature.

We consider that the bath cools down, its temperature continuously evolving with time via some given rule. As the temperature of the bath changes, it leads to a change in the boundary parameterization $f(t)$ that describes the black hole geometry in JT gravity. This in turn modifies the positions of the quantum extremal surface (QES) at different times and hence the Page curve. We compute the modified Page curves numerically.

In more detail, we consider three different cooling profiles— instantaneous temperature drop (for the bath), linear drop in energy, and the temperature following Newton’s law of cooling. For each case, we track the subsequent evolution of the boundary parameterization numerically, starting from the parameterization corresponding to a black hole at temperature β and reaching a temperature $\tilde{\beta}$. Considering the process to be slow enough to remain within the semi-classical regime, we compute the positions of the quantum extremal surfaces and the corresponding entropies at each time step during the process of settling into a new temperature. The results are the Page curves of evaporating black holes in their non-equilibrium phases for each of the three cooling profiles. Note that while we have restricted ourselves to these profiles, the numerical method we use can be utilized for any general case as long as it stays in the semiclassical regime.

*Electronic address: waheed.dar1729@gmail.com

[†]Electronic address: nirmalya@iitmandi.ac.in

[‡]Electronic address: d23189@students.iitmandi.ac.in

In previous literature, a scenario in a somewhat similar spirit was explored in [20], where the modification of the Page curve due to shock waves sent from the bath to the black hole were considered. In this paper, which obtained analytical results, the increase of temperature was assumed to be instantaneous. Our investigations are numerical, which allows us to go beyond these limiting assumptions and investigate the most general cases where the temperature of the bath is changed continuously with time.

The structure and outline of the paper are set out as follows. In Section II, we start with preliminaries and provide the setup. Section III presents the computations for the instantaneous drop in temperature. In section IV, we generalise to more general cooling profiles. Section V. We conclude with a brief summary of the new results.

II. PRELIMINARIES

A. Jackiw-Teitelboim Gravity

Here, we outline the basic aspects of Jackiw-Teitelboim gravity (JT gravity). We refer the reader to [21] for a recent detailed review.

The action of JT gravity minimally coupled to matter is given by:

$$I[g, \Phi] = I_{\text{grav}}[g, \phi] + I_{\text{matter}} \quad (1)$$

Here ϕ denotes the dilatonic field. The gravitational action is given by:

$$I_{\text{grav}}[g, \phi] = \frac{-1}{16\pi G_N} \int_{\mathcal{M}} \sqrt{g} \Phi (R + 2) - \frac{1}{8\pi G_N} \int_{\partial\mathcal{M}} \sqrt{h} \Phi (K - 1) - \frac{\phi_0}{16G_N\pi} \left(\int_{\mathcal{M}} \sqrt{g} R + 2 \int_{\partial\mathcal{M}} \sqrt{h} K \right) \quad (2)$$

The dilaton and the metric equations of motion are given by:

$$R = -2, \quad (3)$$

$$\nabla_{\mu} \nabla_{\nu} \Phi - g_{\mu\nu} \nabla^2 \Phi + g_{\mu\nu} \Phi = -8\pi G_N T_{\mu\nu}. \quad (4)$$

where $T_{\mu\nu}$ is the stress-energy tensor of the matter sector. The dilaton equation of motion constrains the two-dimensional geometry to be locally AdS₂.

B. Quantum Extremal Surfaces

The entropy of Hawking radiation and the generalised entropy are given respectively by the formulae:

$$S_R = \min_I \text{Ext}_I \left[\frac{A(\partial I)}{4G_N} + S_{\text{QFT}}(R \cup I) \right], \quad (5)$$

$$S_{\text{gen}} = \frac{A(\partial I)}{4G_N} + S_{\text{QFT}}(R \cup I). \quad (6)$$

Here, G_N denotes Newton's constant, R is the radiation region, I is the island, ∂I is the boundary of the island, and $S_{\text{QFT}}(R \cup I)$ represents the entanglement entropy of the quantum fields in the bulk region of spacetime. The term $R \cup I$ denotes the union of the island and the radiation region. Extremization of S_{gen} determines the location of the island. The surfaces that extremize the generalised entropy are called quantum extremal surfaces (QES).

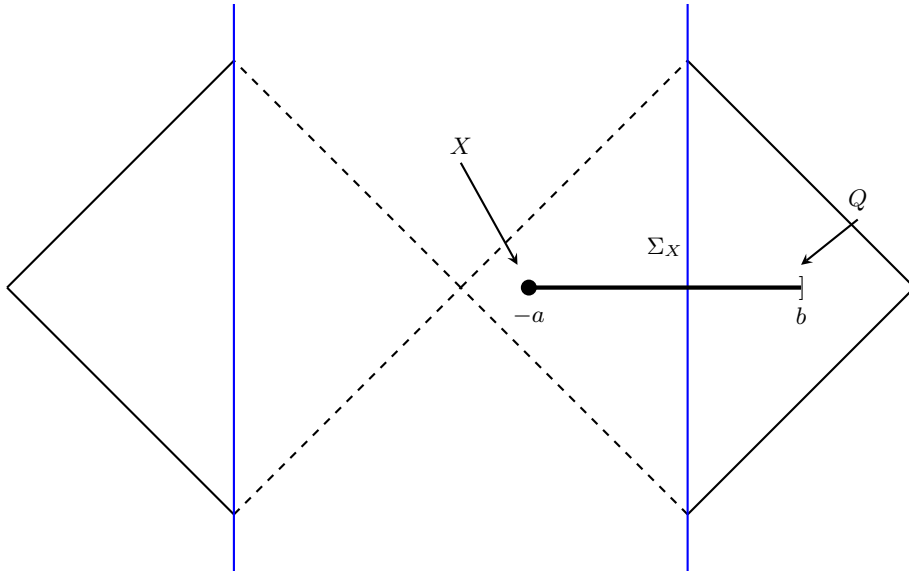


FIG. 1: Quantum Extremal Surface

When there is a non-trivial QES in the bulk, it corresponds to an island. Figure 1 shows a QES where the exact position of ‘a’ is determined by extremization.

C. Black Hole at Equilibrium

1. Geometry

In this section, we briefly introduce the setup. In our case, we have the AdS₂ Poincaré patch with coordinates x^\pm :

$$ds^2 = -\frac{4 dx^+ dx^-}{(x^+ - x^-)^2}. \quad (7)$$

where we have

$$u = \frac{x^+ + x^-}{2} \in \mathbb{R}, \quad s = \frac{x^+ - x^-}{2} > \epsilon$$

The AdS₂ boundary is parametrized by a coordinate transformation $u = f(t)$ which relates the Poincaré coordinates x^\pm to the Rindler coordinates y^\pm . The metric in the y^\pm coordinates is given by:

$$ds^2 = \frac{-4f'(y^+)f'(y^-)}{(f(y^+) - f(y^-))^2} dy^+ dy^- \quad (8)$$

We attach a half-Minkowski thermal bath at the holographic time-like boundary at $z = -\epsilon$. Note that this serves as our IR cut-off. We use flat coordinates for the bath, and we do so by analytically continuing the coordinates of the bulk.

$$ds_{bath}^2 = \frac{-1}{\epsilon^2} dy^+ dy^- \quad (9)$$

An eternal black hole with temperature $\frac{1}{\beta}$ has the boundary parametrization relating the Poincaré and black hole patches given by [20].

$$x^\pm = \frac{\beta}{\pi} \tanh\left(\frac{\pi y^\pm}{\beta}\right) \quad (10)$$

. Then the black hole patch has a metric of the form:

$$ds^2 = -\frac{\pi^2}{\beta^2} \frac{4}{\sinh^2\left(\frac{\pi}{\beta}(y^+ - y^-)\right)} dy^+ dy^-. \quad (11)$$

2. Stress Tensors

The ADM energy of spacetime is holographically related to the boundary parameterization[22]

$$E(t) = -\frac{\phi_r}{8\pi G_N} \{f, t\}, \quad (12)$$

$$\{f(t), t\} \equiv \frac{f'''(t)}{f'(t)} - \frac{3}{2} \left(\frac{f''(t)}{f'(t)} \right)^2. \quad (13)$$

$\{f(t), t\}$ is the Schwarzian derivative of the boundary parametrization. At the boundary, the rate of change of energy is:

$$\frac{\partial E}{\partial t} = T_{y^+y^+} - T_{y^-y^-} \quad (14)$$

Where $T_{y^+y^+}$ is the ingoing stress-energy tensor that originates from the bath attached to the black hole, and $T_{y^-y^-}$ is the outgoing stress-energy tensor, i.e., the Hawking radiation from the black hole.

Under a conformal transformation

$$ds_g^2 = \Omega^{-2} ds_\eta^2$$

The stress-energy tensor components transform as:

$$\langle T_{y^\pm y^\pm} \rangle_g = \langle T_{y^\pm y^\pm} \rangle_\eta - \frac{c}{12\pi} \frac{\partial_\pm^2 \Omega}{\Omega} \quad (15)$$

$$\langle T_{y^\pm y^\pm} \rangle_g = \left(\frac{\partial w^\pm}{\partial y^\pm} \right)^2 \langle T_{w^\pm w^\pm} \rangle_g \quad (16)$$

$$\langle T_{x^\pm x^\pm} \rangle_\eta = \left(\frac{\partial y^\pm}{\partial x^\pm} \right)^2 \langle T_{y^\pm y^\pm} \rangle_\eta + \frac{c}{24\pi} \{x^\pm, y^\pm\} \quad (17)$$

Equation (15) describes a Weyl transformation of the stress-energy tensors, (16) describes the simple tensorial transformation, while (17) represents a coordinate transformation accompanied by a Weyl transformation, respectively.

In the case of an eternal black hole in thermal equilibrium with the radiation bath, both the incoming and outgoing modes of the stress tensor have temperature $\frac{1}{\beta}$

$$\langle T_{y^\pm y^\pm} \rangle = \frac{\pi c}{12\beta^2}, \quad (18)$$

Note that these are expectation values of the normal ordered stress tensor with respect to a flat metric in the respective coordinate.

In equilibrium, we have

$$\frac{\partial E}{\partial t} = 0 \quad (19)$$

We can transform our value of stress tensor using (17), and in doing so, we get $\langle T_{x^\pm x^\pm} \rangle = 0$ as expected

D. Non-Equilibrium

In the previous section, we described a black hole at equilibrium with a heat bath. In this section, we will consider a non-equilibrium situation. In order to create an evaporating black hole, the temperature of the black hole must be higher than that of the bath. In this scenario, radiation can leak into the bath, leading to the evaporation of the black hole.

The change in the bulk geometry because of this is captured in the boundary parameterization in the semi-classical regime, where we assume that there is no back reaction on the geometry.

We start with the bath and the black hole at equilibrium at inverse temperature β and then make a sudden change at boundary time $t = 0$. Before the change, at $t < 0$ or alternately $y^+ < 0$, we have:

$$T_{y^+y^+} = \frac{\pi c}{12\beta^2} \quad (20)$$

Then suddenly the temperature of the bath changes to $\tilde{\beta}$ at the boundary time $t = 0$. This change propagates to the bulk causally. After $y^+ > 0$, we get :

$$T_{y^+y^+} = \frac{\pi c}{12\tilde{\beta}^2} \quad (21)$$

We can express the outgoing stress-energy tensor $T_{y^-y^-}$ as a function of parametrization:

$$T_{y^-y^-} = -\frac{c}{24\pi}\{f(y^-), y^-\}. \quad (22)$$

Energy conservation at the holographic boundary gives from (14):

$$\frac{\partial E}{\partial t} = \frac{\pi c}{12\tilde{\beta}^2} + \frac{c}{24\pi}\{f(t), t\} \quad (23)$$

Upon substituting the parameterization with E, we get:

$$\frac{\partial E}{\partial t} = \frac{\pi c}{12\tilde{\beta}^2} - \frac{G_N c}{3\phi_r} E \quad (24)$$

$$E = e^{-kt} \int \left[\frac{\pi c}{12\tilde{\beta}^2} e^{kt} dt \right] \quad (25)$$

Where $k = \frac{G_N c}{3\phi_r}$.

We solve this differential equation with the boundary condition that at $t = 0$ the ADM energy is $E = \frac{\pi\phi_r}{4\beta^2 G_N}$, which was the original energy of the black hole before any evaporation took place. The third-order differential equation for boundary parametrization is obtained as:

$$\{f, t\} = -2\pi^2[\tilde{\beta}^{-2} - (\tilde{\beta}^{-2} - \beta^{-2})e^{-kt}].$$

This is solved in [6][20] where the solution for boundary parameterization comes out to be modified Bessel functions. Note we fix $k \ll 1$ in order to work in the semi-classical regime. In our case, $k = 0.05$, and also the time step for evolution is 0.01.

However, we generally proceed with the differential equation and solve it numerically. This numerical solution allows us the flexibility to solve some other variations of this differential equation that are not solvable by analytical methods. Our result for a single sudden change in temperature of the bath is analogous to the result [20] where the black hole evaporates from one temperature and settles down to another. Although the physical process remains the same in both cases, our numerical approach allows for both the $w\pm$ coordinates to change and fine-tuning of the temperature change profile, whereas the result [20] is analytical in nature and for a single instant change in temperature of the black hole using a shockwave. This keeps the bath temperature constant throughout the analysis, thereby only changing the outgoing ‘w’ coordinate.

E. Early Times and Late Times

In early times, the black hole was in equilibrium with the bath at temperature T_β , and we are interested in black hole evaporation at very late times when the black hole has reached equilibrium with the bath at temperature $T_{\tilde{\beta}}$. Solving the differential equation numerically with the appropriate boundary condition results in interpolation between the initial and final parameterization, which is what we expected.

Initially:

$$f(y^\pm) = \frac{\beta}{\pi} \tanh\left(\frac{\pi}{\beta} y^\pm\right) \quad (26)$$

$$f'(y^\pm) = \text{sech}^2\left(\frac{\pi}{\beta} y^\pm\right) \quad (27)$$

$$f''(y^\pm) = -\frac{2\pi}{\beta} \sinh\left(\frac{\pi}{\beta} y^\pm\right) \text{sech}^3\left(\frac{\pi}{\beta} y^\pm\right) \quad (28)$$

At very late times, it should approximate:

$$f(y^\pm) \approx \frac{\tilde{\beta}}{\pi} \tanh\left(\frac{\pi}{\tilde{\beta}} y^\pm\right) \quad (29)$$

$$f'(y^\pm) = \text{sech}^2\left(\frac{\pi}{\tilde{\beta}} y^\pm\right) \quad (30)$$

$$f''(y^\pm) = -\frac{2\pi}{\tilde{\beta}} \sinh\left(\frac{\pi}{\tilde{\beta}} y^\pm\right) \text{sech}^3\left(\frac{\pi}{\tilde{\beta}} y^\pm\right) \quad (31)$$

From Figure 2 and 3, it can be seen how the derivative and double derivative of the boundary parameterization interpolate between the old and very late times (new) boundary parameterizations.

III. EVAPORATION OF BLACK HOLE: INSTANTANEOUS CHANGE IN BATH TEMPERATURE

In this section, we present our computations for black hole evaporation when the temperature of the bath drops instantaneously. The evaporation of the black hole and its dynamics are captured in the parameterization, which interpolates between the old and new parameterizations. We track the evolution of the entropy of the black hole using (5) and obtain the Page curve of an evaporating black hole. The entropy is calculated numerically for the Hawking Saddle and the Island Saddle. We evaporate the black hole by decreasing the temperature of the bath and breaking the equilibrium.

First, we introduce a new frame w^\pm where the CFT is in a vacuum state with a flat background geometry:

$$\langle T_{w^\pm w^\pm} \rangle = 0 \quad (32)$$

In this frame, the matter entanglement entropy between two points a and b is given by the Cardy-Calabrese formula [23]:

$$S = \frac{c}{6} \log \left| \frac{(w_a^+ - w_b^+)(w_a^- - w_b^-)}{\epsilon^{w_a^+} \epsilon^{w_a^-} \epsilon^{w_b^+} \epsilon^{w_b^-}} \right|. \quad (33)$$

Here, $\epsilon^{w_a^+}, \epsilon^{w_a^-}, \epsilon^{w_b^+}, \epsilon^{w_b^-}$ are the UV cutoffs for the entropy at points a and b . The cut-offs are taken with respect to the proper distance in the physical metric. Saddles.

Now we want to relate the w -frame to the original coordinate system y . The stress energy tensor in the two frames is related by:

$$\left(\frac{dw^\pm}{dy^\pm}\right)^2 \langle T_{w^\pm w^\pm} \rangle = \langle T_{y^\pm y^\pm} \rangle + \frac{c}{24\pi} \{w^\pm, y^\pm\} \quad (34)$$

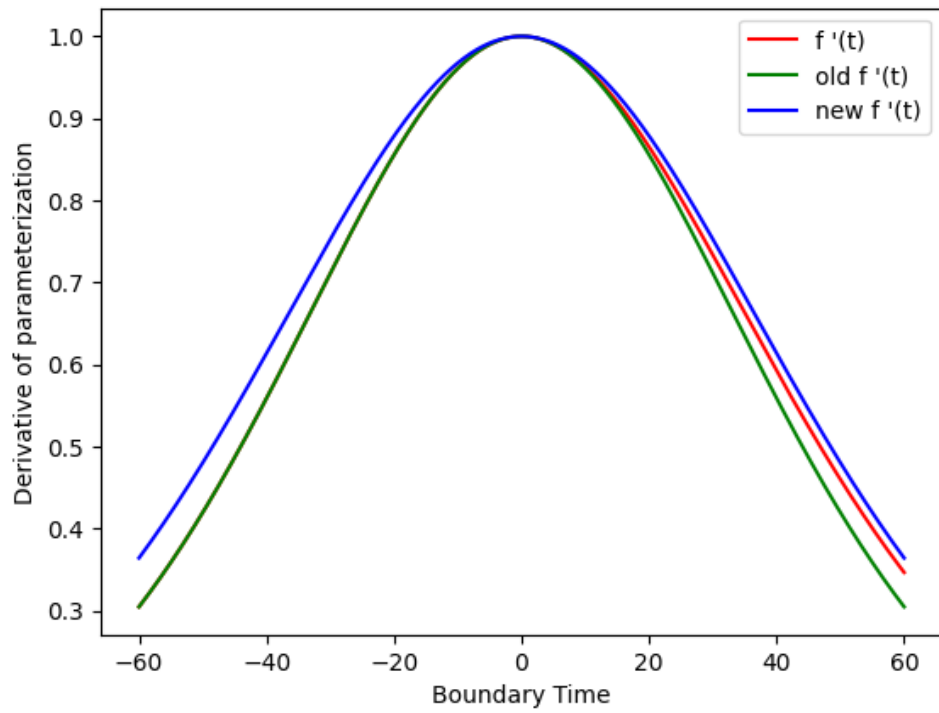


FIG. 2: Plot of first derivative of $f(u)$ with u

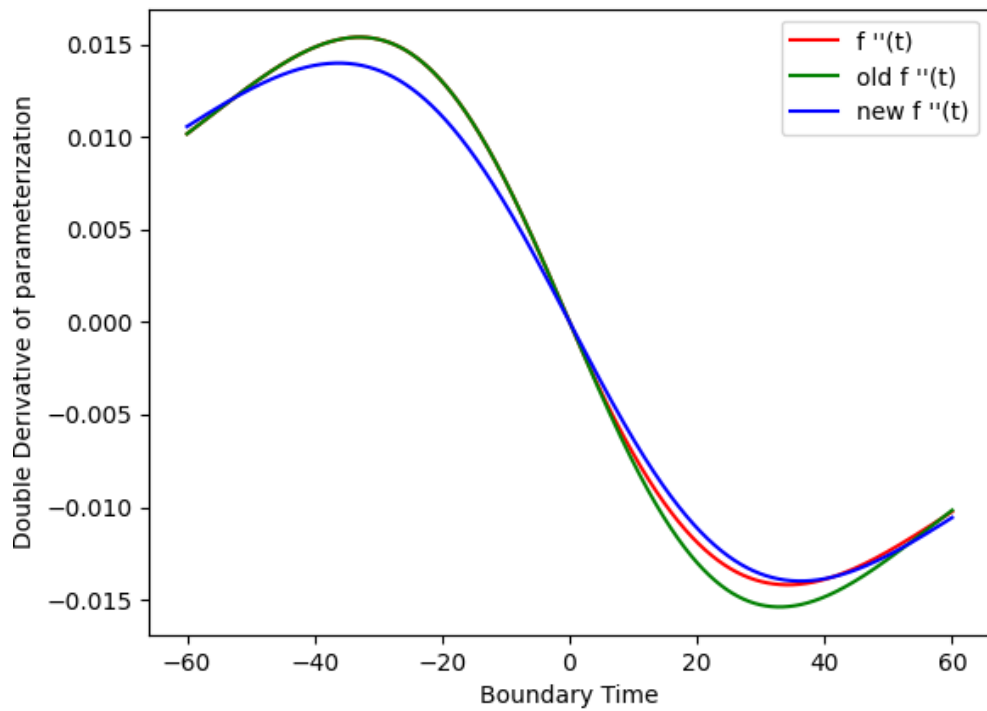


FIG. 3: Plot of second derivative of $f(u)$ with u

First, consider the coordinate w^+ .

We have from (32) and (34):

$$\{w^+, y^+\} = -\frac{24\pi}{c} \langle T_{y^+y^+} \rangle, \quad (35)$$

Combining this with (20), we get:

$$\{w^+, y^+\} = -\frac{2\pi^2}{\beta^2}, \quad y^+ < 0, \quad (36)$$

$$(37)$$

Likewise, from (21):

$$\{w^+, y^+\} = -\frac{2\pi^2}{\beta^2}, \quad y^+ \geq 0 \quad (38)$$

During $y^+ < 0$, $w^+ = e^{\frac{2\pi}{\beta}y^+}$ solves (36) and provides a coordinate system for both the black hole and the bath. After $y^+ = 0$, the coordinate relation between y^+ and w^+ is to be obtained by solving (38).

As (38) is a third-order differential equation, we have to specify three initial conditions at $y^+ = 0$. We impose continuity in the w^+ coordinates up to the second-order derivative. This gives us:

$$\begin{aligned} w^+|_{y^+=0} &= 1 \\ \frac{dw^+}{dy^+}|_{y^+=0} &= \frac{2\pi}{\beta} \\ \frac{d^2w^+}{dy^{+2}}|_{y^+=0} &= \frac{4\pi^2}{\beta^2} \end{aligned}$$

The discontinuous change in the bath temperature is reflected as the discontinuity of the Schwarzian, which shows up in the third-order derivative. This discontinuity is an artifact of our rather artificial assumption of a discontinuous change in the bath temperature.

A similar argument follows for w^- coordinates, where we have

$$\langle T_{y^-y^-} \rangle = \frac{\pi c}{12\beta^2}, \quad y^- < 0, \quad \langle T_{y^-y^-} \rangle = \frac{\pi c}{12} \left[\frac{1}{\tilde{\beta}^2} - \left(\frac{1}{\tilde{\beta}^2} - \frac{1}{\beta^2} \right) e^{-kt} \right] \quad y^- \geq 0 \quad (39)$$

It follows that for $y^- < 0$, the relation between y^- and w^- has the same form as (36):

$$\{w^-, y^-\} = -\frac{2\pi^2}{\beta^2}, \quad y^- < 0 \quad (40)$$

Which is solved by $w^- = -e^{-\frac{2\pi}{\beta}y^-}$.

For $y^- \geq 0$ the form of the relation is different from (38), however:

$$\{w^-, y^-\} = -2\pi^2 \left[\tilde{\beta}^{-2} - \left(\tilde{\beta}^{-2} - \beta^{-2} \right) e^{-kt} \right], \quad y^- \geq 0 \quad (41)$$

Here too, we choose initial conditions that ensure continuity up to the second order derivative:

$$\begin{aligned} w^-|_{y^+=0} &= -1 \\ \frac{dw^-}{dy^-}|_{y^+=0} &= \frac{2\pi}{\beta} \\ \frac{d^2w^-}{dy^{-2}}|_{y^+=0} &= -\frac{4\pi^2}{\beta^2} \end{aligned}$$

Unlike in the previous case, here the Schwarzian is no longer discontinuous. This reflects the fact that although the

bath temperature changes suddenly, the black hole temperature changes in a continuous manner.

The cut-off distances in (33) are taken in terms of the physical metric, which is ϵ^{y^\pm} . In the w-frame, these are given by:

$$\epsilon^{w^+} \epsilon^{w^-} = -dw^+ dw^- \quad (42)$$

$$-dw^+ dw^- = -dy^+ dy^- \left(\frac{dy^+}{dw^+} \right) \left(\frac{dy^-}{dw^-} \right) \quad (43)$$

$$-dw^+ dw^- = -\Omega^2 dy^+ dy^- \left(\frac{dy^+}{dw^+} \right) \left(\frac{dy^-}{dw^-} \right) \frac{1}{\Omega^2} \quad (44)$$

$$-dw^+ dw^- = \epsilon^{y^+} \epsilon^{y^-} \left(\frac{dy^+}{dw^+} \right) \left(\frac{dy^-}{dw^-} \right) \frac{1}{\Omega^2} \quad (45)$$

$$\epsilon^{w^+} \epsilon^{w^-} = \epsilon^{y^+} \epsilon^{y^-} \left(\frac{dy^+}{dw^+} \right) \left(\frac{dy^-}{dw^-} \right) \frac{1}{\Omega^2} \quad (46)$$

The blackening factor Ω^2 for the metric in the y-frame is given by:

$$\Omega^2 = \frac{-4f'(y^+)f'(y^-)}{(f(y^+) - f(y^-))^2} \quad (47)$$

Where f is the boundary parameterization function. Note that for the point a in the bulk, Ω^2 varies, but for the point b in the bath, it is a constant.

Next, we fix the dilaton. In the semi-classical limit, the dilaton is obtained by solving the dilaton equation (4). We solve it in the x^\pm frame and then relate the result to the y^\pm frame using $x^\pm = f(y^\pm)$. To do this, we first determine $\langle T_{x^\pm x^\pm} \rangle$. From (17), we see that $\langle T_{x^+ x^-} \rangle$ and $\langle T_{x^- x^+} \rangle$ both vanish. The non-zero component $\langle T_{x^+ x^+} \rangle$ is given by:

$$T_{x^+ x^+} = \frac{1}{f'(y^+)^2} \left(\frac{\pi c}{12\beta^2} + \frac{c}{24\pi} \{f(y^+), y^+\} \right).$$

From (23), this equals:

$$T_{x^+ x^+} = \frac{1}{f'(y^+)^2} \partial_{y^+} E(y^+) = -\frac{\phi_r}{8\pi G_N} \frac{1}{f'(y^+)^2} \partial_{y^+} \{f(y^+), y^+\}$$

Using $\{f^{-1}(x^+), x^+\} = -(f'(y^+))^{-2} \{f(y^+), y^+\}$, we get:

$$T_{x^+ x^+} = -\frac{\phi_r}{8\pi G_N} \partial_{x^+}^3 f'(y^+)$$

Now we follow the argument as in [20] to obtain the expression for the dilaton:

$$\phi = \phi_0 + 2\phi_r \left(\frac{f''(y^+)}{2f'(y^+)} + \frac{f'(y^+)}{f(y^-) - f(y^+)} \right)$$

Now we are ready to calculate the entropy using the Island formulae (5) and (6).

A. Hawking saddle

We start with the calculation of the trivial Hawking saddle.

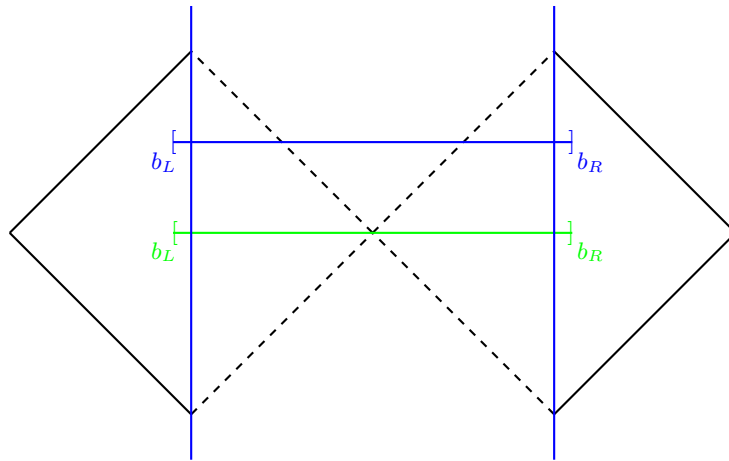


FIG. 4: Hawking saddle represented geometrically. Entropy is related to the proper distance between the two points.

Before calculating, we need to figure out the w^\pm coordinates for both endpoints b_L and b_R (as shown in Figure 4). We start by specifying the points in the y frame and then write them in the w -frame coordinates. In the y -frame, we fix the spatial distance of the points from the cutoff surface. We fix $z = 2\epsilon$, so at any boundary time t the y^\pm coordinates of the points in the right bath are:

$$y^+ = (t + z)/2, \quad y^- = (t - z)/2 \quad (48)$$

$$(49)$$

We proceed similarly for the left side bath and get these points in the corresponding w^\pm coordinates. Note that the w^\pm coordinates that we use to completely span the two-sided black hole, along with the two baths attached on either side. Then the Hawking saddle is the entanglement entropy between the two bath points using Cardy-Calabrese formulae.

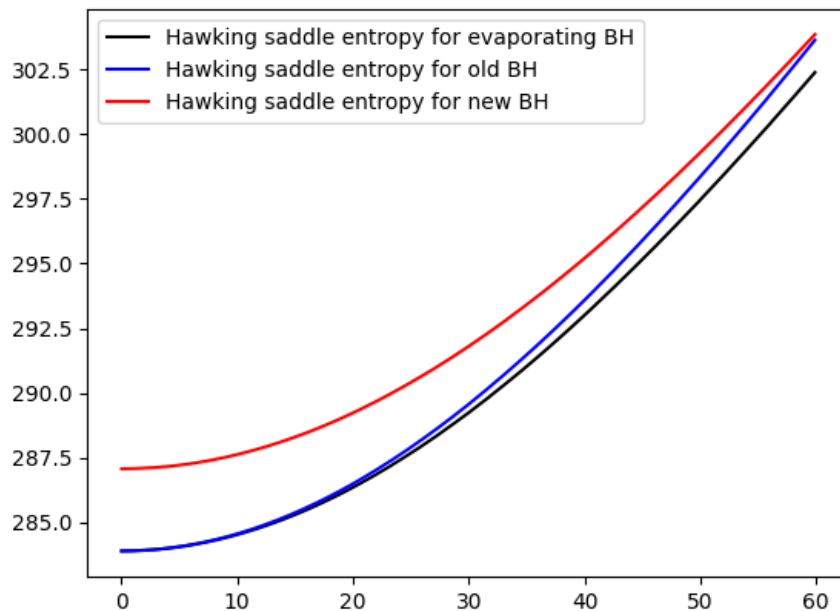


FIG. 5: Entropy of Hawking saddle vs Boundary time

In Figure 5, the entropy curves corresponding to the old and new black holes are the Hawking saddle entropy curve for eternal black holes corresponding to the initial and final temperature, respectively. It can be seen that the entropy curve for our evaporating black hole starts as the old one but later becomes parallel to the new saddle. As expected, the Hawking saddle entropy curve becomes linear at late times, with slope proportional to the temperature of the black hole. We have now obtained the graph for our evaporating black hole, which shows a clear interpolation between the initial and final state.

B. Island saddle

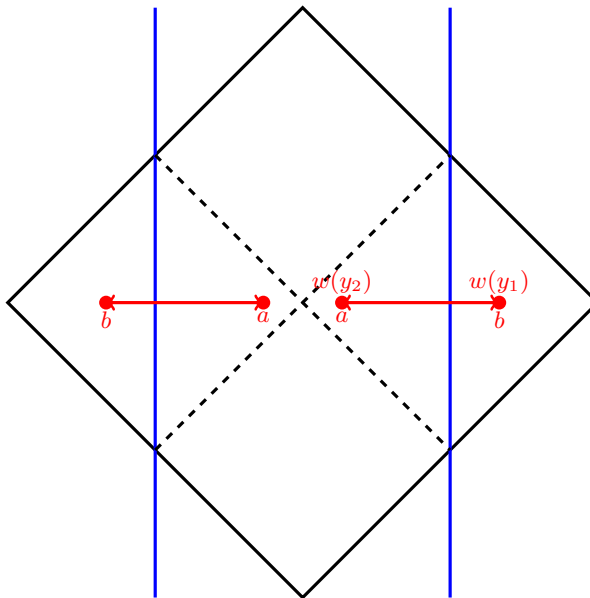


FIG. 6: Geometric representation of island saddle. Entropy is related to the proper distance along the red lines and the value of dilaton at ‘a’. The points ‘a’ are QES in respect to the points ‘b’.

In the island saddle calculation, we iterate over all possible points ‘a’ (‘ y_2 ’ in the above diagram 6) in a fixed time slice to find an extrema. Note that there is a symmetry between the left and the right side of the diagram.

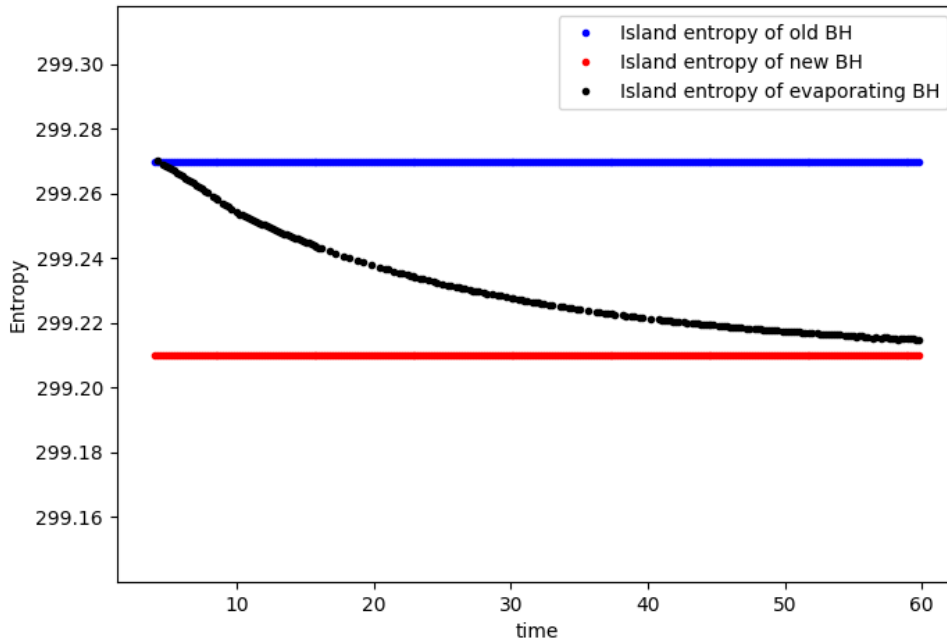


FIG. 7: Entropy of Island saddle vs Boundary time

Figure 7 shows the decrease in island entropy over time from the black hole entropy corresponding to the black hole at the initial temperature to that corresponding to a black hole at the new temperature. The asymptotic behavior of the black hole coming to equilibrium in its final state is clearly reflected in the graph. As expected, the Page curve comes down for an evaporating black hole, whereas it stays at a constant value for an eternal black hole. Thus, we have directly obtained the Page curve after Page time for an evaporating black hole. Further, this numerical approach can be used to profile evaporation for any type of cooling that the bath might provide.

IV. BLACK HOLE EVAPORATION: GENERAL COOLING PROFILES

In this section, we explore different examples of cooling of the bath, which are continuous in nature and different from the earlier delta function drop in temperature.

The starting point for the general case is the generalization of (23):

$$\frac{\partial E}{\partial t} = \frac{\pi c}{12\tilde{\beta}_t^2} + \frac{c}{24\pi} \{f(t), t\} \quad (50)$$

where $\tilde{\beta}_t^2$ is the temperature of the bath.

We will focus on three examples: a case where the bath temperature follows Newton's law of cooling, one where the incoming stress tensor from the bath has a drop in value linear in time, and finally, a quasi-static case.

A. Bath Energy follows Newton's law of cooling

In this case, we take $\frac{\pi c}{12\tilde{\beta}_t^2} = \frac{\pi c}{12} \left(\frac{1}{\tilde{\beta}^2} + \left(\frac{1}{\tilde{\beta}^2} - \frac{1}{\tilde{\beta}^2} \right) e^{-st} \right)$. We choose s to be the cooling constant. We solve for E and then solve for boundary parameterization. The rest of the machinery works similarly, replacing $\tilde{\beta}$ with $\tilde{\beta}_t$.

Finally, we want to see how the black hole entropy and the island entropy change with time for different values of s and k . We mainly have three cases: $k > s$, $k < s$, and $k = s$. We also see how the energy of this black hole changes.

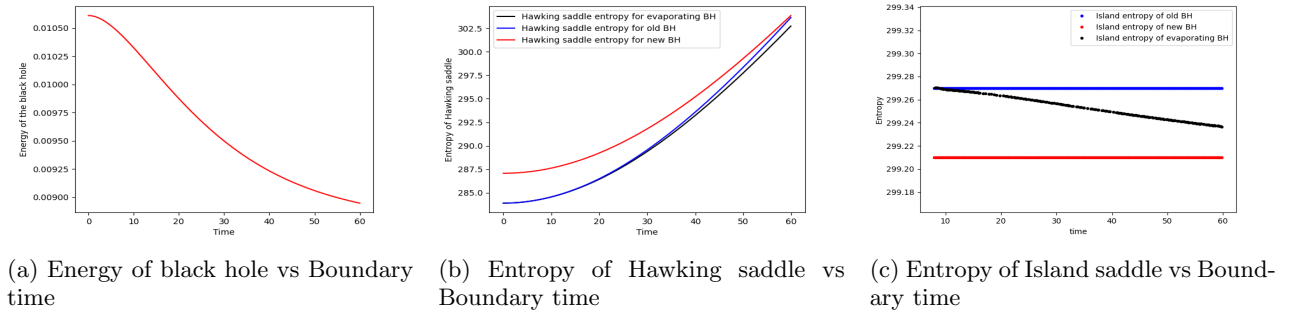
FIG. 8: Case 1: $k > s$

Figure 8a8b8c corresponds to Energy, Hawking saddle entropy, and Island saddle entropy, respectively. We see that the island entropy curve is slightly concave at early times and nearly flat at late times.

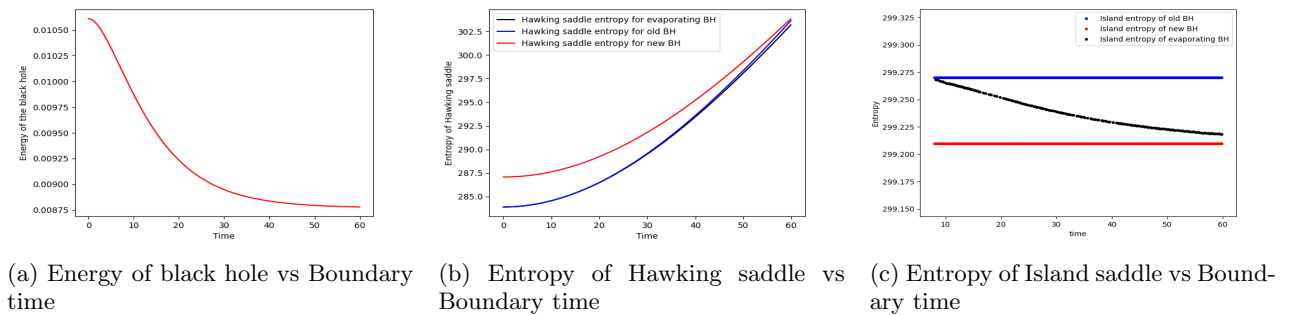
FIG. 9: case 2: $k < s$

Figure 9a9b9c corresponds to Energy, Hawking saddle entropy, and Island saddle entropy, respectively. We can see that the island entropy curve is nearly flat at early times and convex at late times.

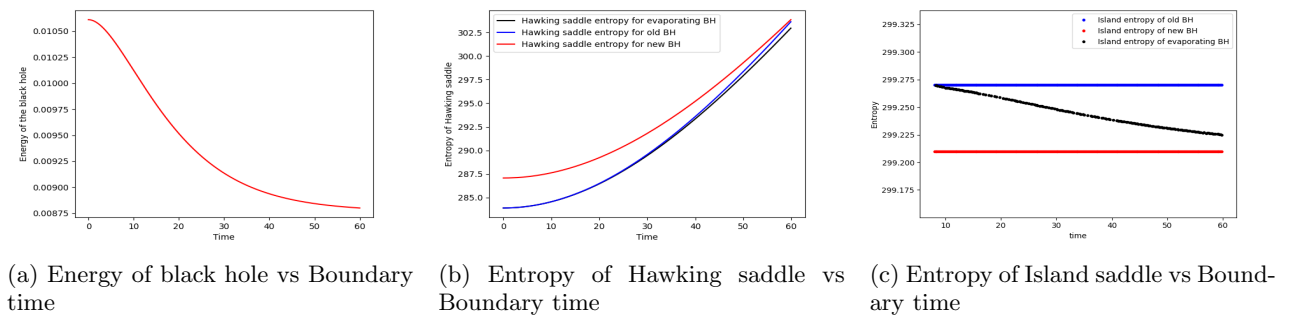
FIG. 10: Case 3: $k = s$

Figure 10a10b10c corresponds to Energy, Hawking saddle entropy, and Island saddle entropy, respectively. We find that the island entropy curve is slightly concave at early times and slightly convex at late times.

B. Linear Decrease in Incoming Stress Tensor.

In this case, we take $\frac{\pi c}{12\beta_t^2} = \frac{\pi c}{12\beta^2} - st$. Here s is the rate of decay in incoming energy. We follow the same procedure to calculate the island entropy for this evaporation profile. Here, the black hole energy as a function of time is initially concave and later becomes straight.

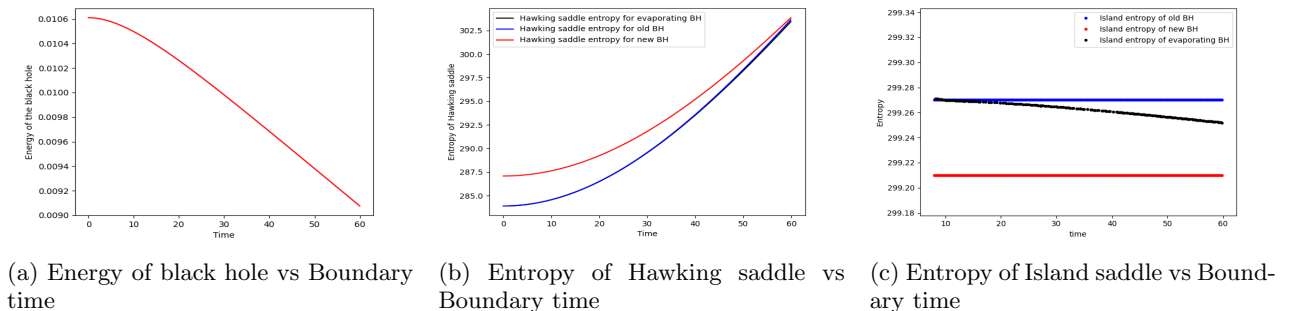


FIG. 11: Linear decrease in bath stress tensor

Figure 11a11b11c corresponds to Energy, Hawking saddle entropy, and Island saddle entropy, respectively. We find the entropy curve to be slightly concave throughout. We do not expect the curve to be convex at later times, as there is no final temperature to settle in.

C. Quasi-static Evaporation

We would like to compare the results from the different models of evaporation to one where the cooling is quasi-static, with equilibrium being maintained at each time step. We model this by treating the black hole as an eternal black hole at temperature β_t at each time step, with β_t taken to be a constant during the timestep. The incoming and outgoing stress tensors are taken as the same function, thereby always ensuring equilibrium.

We can then vary β_t as we like, and the entropy curve obtained will represent the island entropy for a quasi-static evolution. We take $\frac{1}{\beta_t^2} = \left(\frac{1}{\beta^2} + \left(\frac{1}{\beta^2} - \frac{1}{\beta^2}\right)e^{-kt}\right)$. This temperature profile corresponds to the temperature of a black hole evaporating due to a single sudden change in bath temperature thereby breaking equilibrium. If we take this same temperature profile for a black hole evaporating in a quasi-static manner, it corresponds to cooling like Newton's Law of Cooling for both the bath and the black hole.

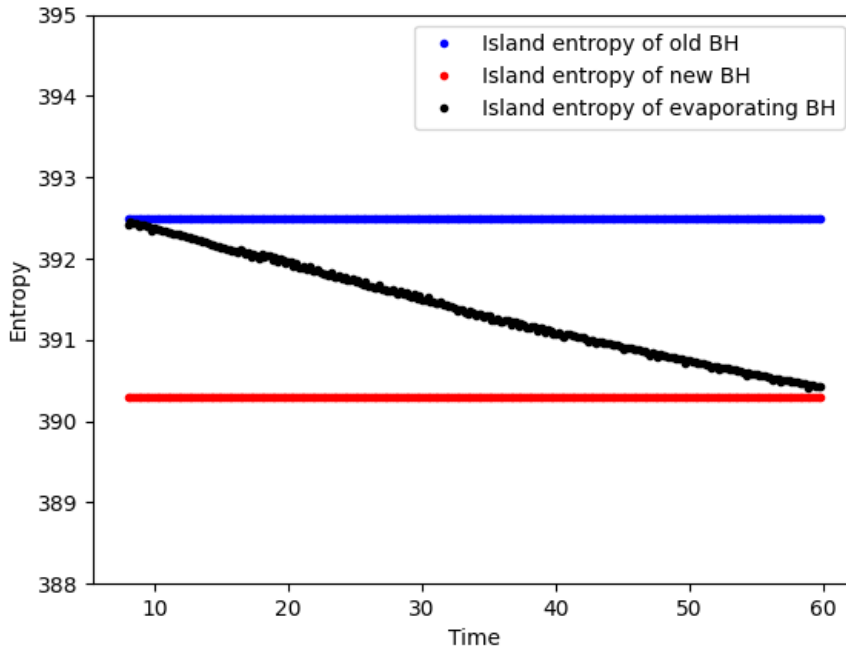


FIG. 12: Entropy of Hawking saddle vs Boundary time

Comparing Figure 12 with Figure 7, we see that the quasi-static evolution is a much faster decay. The difference in the numerical values of island entropy for the initial and final temperature is also much larger in magnitude. Note that this Figure 12 is for $k = 0.01$, whereas for Figure 7, $k = 0.1$. The value of k directly correlates to the rate of change of temperature of the black hole. Even so, with a lower k , the drop in value for the island entropy for the quasi-static case is substantially more than that of a dynamically evaporating black hole.

As mentioned previously, the purpose of including this non-dynamical case is to provide a point of comparison for our previous results.

V. CONCLUSION

In this paper, we extended previous results on Page curves for evaporating black holes in JT gravity to the general case where the bath temperature can be controlled externally.

Using the Island formula, we tracked the Hawking and the Island saddle entropy numerically for an evaporating black hole. Unlike the previous discussions where a black hole was given a shock, and its evaporation back to its original state was studied, our approach is more general. We continuously change the bath temperature and consider several different profiles of continuous temperature change. In this paper, we studied three profiles: linear change, Newton's law of cooling, and step function cooling. The result gives the Page curves of a slowly evaporating black hole in AdS under different external conditions of cooling, while remaining in the semiclassical regime.

Our numerical methods are entirely general and can then be used to study any cooling profile of the bath. We leave this to future investigations.

Physically, our result is expected to be useful in modeling black hole evaporation under general external conditions. Non-trivial environments can affect the evaporation of black holes. Our methods show how to track the evolution of the Page curve under such general conditions.

VI. ACKNOWLEDGMENTS

NK was supported by the SERB Start-up Research Grant SRG/2022/000970 during a significant part of this research.

-
- [1] Don N. Page. Average entropy of a subsystem. *Phys. Rev. Lett.*, 71:1291–1294, 1993.
 - [2] Ahmed Almheiri, Raghunathan Mahajan, Juan Maldacena, and Ying Zhao. The Page curve of Hawking radiation from semiclassical geometry. *JHEP*, 03:149, 2020.
 - [3] Geoffrey Penington. Entanglement Wedge Reconstruction and the Information Paradox. *JHEP*, 09:002, 2020.
 - [4] Netta Engelhardt and Aron C. Wall. Quantum Extremal Surfaces: Holographic Entanglement Entropy beyond the Classical Regime. *JHEP*, 01:073, 2015.
 - [5] Geoff Penington, Stephen H. Shenker, Douglas Stanford, and Zhenbin Yang. Replica wormholes and the black hole interior. *JHEP*, 03:205, 2022.
 - [6] Ahmed Almheiri, Thomas Hartman, Juan Maldacena, Edgar Shaghoulian, and Amirhossein Tajdini. Replica Wormholes and the Entropy of Hawking Radiation. *JHEP*, 05:013, 2020.
 - [7] Ahmed Almheiri, Thomas Hartman, Juan Maldacena, Edgar Shaghoulian, and Amirhossein Tajdini. The entropy of Hawking radiation. *Rev. Mod. Phys.*, 93(3):035002, 2021.
 - [8] Ahmed Almheiri, Raghunathan Mahajan, and Juan Maldacena. Islands outside the horizon. 10 2019.
 - [9] Donald Marolf and Henry Maxfield. Transcending the ensemble: baby universes, spacetime wormholes, and the order and disorder of black hole information. *JHEP*, 08:044, 2020.
 - [10] Ahmed Almheiri, Raghunathan Mahajan, and Jorge E. Santos. Entanglement islands in higher dimensions. *SciPost Phys.*, 9(1):001, 2020.
 - [11] Hong Zhe Chen, Robert C. Myers, Dominik Neuenfeld, Ignacio A. Reyes, and Joshua Sandor. Quantum Extremal Islands Made Easy, Part I: Entanglement on the Brane. *JHEP*, 10:166, 2020.
 - [12] Koji Hashimoto, Norihiro Iizuka, and Yoshinori Matsuo. Islands in Schwarzschild black holes. *JHEP*, 06:085, 2020.
 - [13] Thomas Hartman, Yikun Jiang, and Edgar Shaghoulian. Islands in cosmology. *JHEP*, 11:111, 2020.
 - [14] Fridrik Freyr Gautason, Lukas Schneiderbauer, Watsé Sybesma, and Larus Thorlacius. Page Curve for an Evaporating Black Hole. *JHEP*, 05:091, 2020.
 - [15] Vijay Balasubramanian, Arjun Kar, and Tomonori Ugajin. Islands in de Sitter space. *JHEP*, 02:072, 2021.
 - [16] Chethan Krishnan. Critical Islands. *JHEP*, 01:179, 2021.
 - [17] Chethan Krishnan, Vaishnavi Patil, and Jude Pereira. Page Curve and the Information Paradox in Flat Space. 5 2020.
 - [18] Yi Ling, Yuxuan Liu, and Zhuo-Yu Xian. Island in Charged Black Holes. *JHEP*, 03:251, 2021.
 - [19] Byoungjoon Ahn, Sang-Eon Bak, Hyun-Sik Jeong, Keun-Young Kim, and Ya-Wen Sun. Islands in charged linear dilaton black holes. *Phys. Rev. D*, 105(4):046012, 2022.
 - [20] Timothy J. Hollowood and S. Prem Kumar. Islands and Page Curves for Evaporating Black Holes in JT Gravity. *JHEP*, 08:094, 2020.
 - [21] Thomas G. Mertens and Gustavo J. Turiaci. Solvable models of quantum black holes: a review on Jackiw–Teitelboim gravity. *Living Rev. Rel.*, 26(1):4, 2023.
 - [22] Juan Maldacena, Douglas Stanford, and Zhenbin Yang. Conformal symmetry and its breaking in two dimensional Nearly Anti-de-Sitter space. *PTEP*, 2016(12):12C104, 2016.
 - [23] Pasquale Calabrese and John L. Cardy. Entanglement entropy and quantum field theory. *J. Stat. Mech.*, 0406:P06002, 2004.